



# Recent advances in the application of carbon-based electrode materials for high-performance zinc ion capacitors: a mini review

Yongpeng Ma<sup>1</sup> · Chuanxin Hou<sup>1</sup> · Hideo Kimura<sup>1</sup> · Xiubo Xie<sup>1</sup> · Huiyu Jiang<sup>1</sup> · Xueqin Sun<sup>1</sup> · Xiaoyang Yang<sup>1</sup> · Yuping Zhang<sup>1</sup> · Wei Du<sup>1</sup>

Received: 4 January 2023 / Revised: 8 February 2023 / Accepted: 28 February 2023 / Published online: 9 March 2023  
© The Author(s), under exclusive licence to Springer Nature Switzerland AG 2023

## Abstract

Designing and developing advanced energy storage equipment with excellent energy density, remarkable power density, and outstanding long-cycle performance is an urgent task. Zinc-ion hybrid supercapacitors (ZIHCs) are considered great potential candidates for energy storage systems due to the features of high power density, stable cycling lifespans, high safety, low cost, and long-term durability, which originate from the combination of the dual advantages of supercapacitors and zinc-ion batteries. Recently, to pursue the long lifespan of ZIHCs, effective progress has been made in the development and application of ZIHC cathode materials based on carbon-based materials. This review takes carbon-based materials as the starting point and discusses the charge storage mechanism of ZIHCs. Moreover, the application of various carbon-based materials is systematically summarized in ZIHCs, including activated carbon (AC), biomass carbon (BC), porous carbon (PC), and heteroatom-doped carbon (HDC). In addition, recent advances in the structural design of electrolytes and Zn anodes and their effects on electrochemical performance are summarized. Ultimately, the current challenges and the potential directions for ZIHCs are presented. This paper intends to provide directions for the further development of high-performance ZIHCs.

**Keywords** Zinc-ion hybrid supercapacitor · Carbon-based electrodes · Electrochemical performance

## 1 Introduction

The sustainable development goals of modern society have prompted the world to focus on conserving energy resources and implementing a comprehensive conservation strategy [1–7]. The rapid development and utilization of new and recyclable energy sources, including solar energy and wind energy, impels the exploration of energy storage devices, such as batteries and supercapacitors [8–14]. The electrochemical performance of different storage devices generally depends on their energy storage mechanism. The cell undoubtedly has excellent energy storage capacity, with the cation departing from the cathode into the electrolyte and

then adsorbing/inserting itself into the anode. During discharge, they are then un-inserted from the anode into the electrolyte and returned to the cathode. At the same time, the anion moves from the electrolyte and adsorbs onto the anode. However, the slow energy storage rate results in high energy density but low power density. Unlike batteries, supercapacitors (especially electric double-layer capacitors) absorb charge at the surface of the electrode material, and the ions in the electrolyte move toward the positive and negative electrodes, respectively, during charging, thus allowing reversible charging and discharging processes at very fast speeds with the high power density and low energy density [15, 16]. Furthermore, the characteristic ultralong cycling performance of supercapacitors is superior to batteries, which is irreplaceable in practical applications that require high power density and ultralong cycle capability, such as airplanes and powered cars [17]. Nevertheless, the practical widely application was hindered based on its low energy density [18–21]. Consequently, multitudinous strategies have been carried out to enhance the energy density based on the advantages of high power density and ultralong cycling stability to broaden its application fields [22–24].

✉ Chuanxin Hou  
chuanxin210@ytu.edu.cn

✉ Wei Du  
duwei@ytu.edu.cn

<sup>1</sup> School of Environmental and Material Engineering,  
Yantai University, No. 30 Qingquan Road, Yantai,  
Shandong 264005, China

The energy density for the supercapacitor is calculated via Eq. (1):

$$E = \frac{1}{2} CV^2 \quad (1)$$

where  $E$  represents the energy density,  $C$  signifies the specific capacitance of the active material, and  $V$  means the working voltage. Obviously, the energy density of supercapacitors can be enhanced mainly according to the improvement of the capacity of the active material and the operating voltage. In addition to optimizing electrolytes, designing and building special structures of capacitor devices, especially combining the advantages of capacitor-type electrodes with battery-type electrodes, is believed to be effective to improve its working voltage for obtaining the ideal performance of supercapacitors [25–28].

Among the multitudinous research, metallic Zn has been chosen as an excellent anode electrode for supercapacitors systems due to its superiority of low standard potential, high security, low cost, environmental protection, and mass production. The zinc-ion hybrid supercapacitors (ZIHCs) consist of the superiority of supercapacitors and Zn-ion batteries, with Zn sheets as negative electrodes to broaden the operating voltage, which was believed to have immense potential in improving the low energy density of conventional supercapacitors [29–31]. The concept of ZIHCs with carbon nanotubes and metallic Zn as electrode materials was creatively put forward in 2016, which delivered a capacitance of  $53 \text{ F g}^{-1}$  [32], setting off a research boom in ZIHCs. A high capacitance of  $436 \text{ F g}^{-1}$  and long-cycle stability of ZIHCs using carbon-based electrode materials was achieved in a recent study [33], which shows a bright, practical application prospect of ZIHCs in terms of carbon-based cathodes.

Besides numerous explorations on Zn-anode protection, enormous attention has been paid to carbon-based cathode materials that store charge through electrochemical double layers (EDLC) and pseudo-capacitance effects [34]. EDLC capacitance relies on their rich specific surface area and pore structure that allows extensive active site contact between electrolyte ions and the carbon cathode, while the pseudo-capacitance capacitance is related to the surface functional groups of the cathode material or the occurrence of redox reactions. Therefore, the design of carbon-based nanostructures with large specific surface area or/and by introducing heteroatoms [35], conducting polymers [36], organic molecules [37], and metal oxides [38] are essential for the enhancement of EDLC and pseudo-capacitance property.

In this review, the research progress and challenges of ZIHCs were presented, which can be summarized in Fig. 1. The principle of ZIHC, mainly including the energy storage

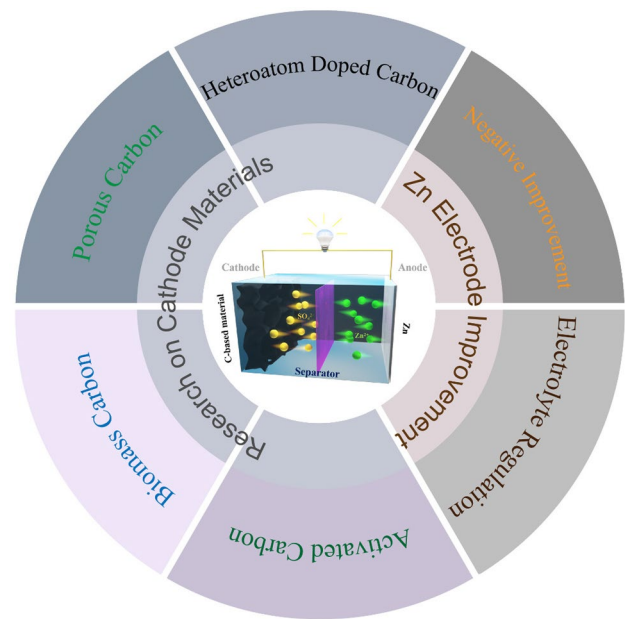


Fig. 1 Summary of the aspects discussed in this review

mechanism and energy calculation method, is first introduced. Then, the research progress of ZIHCs with carbon-based cathode materials is comprehensively described, such as the improvement project of activated carbon, biomass carbon, and other materials. Besides, the effects of electrode structure design and emerging electrolyte systems on the electrochemical performance of ZIHCs are reviewed. Finally, the technological challenges and the future development direction of ZIHCs are discussed. This review will offer a more profound perception of carbon-based electrodes for ZIHCs and assists with technological innovation.

## 2 Energy storage mechanisms of ZIHCs

Theoretically, the capacity of ZIHCs is considered to have no upper limit due to the negative zinc electrode exhibiting Faraday capacitance and a flat potential platform. Therefore, the capacitance of ZIHCs almost entirely originates from the contribution of carbon materials (Eq. (2)); meanwhile, ZIHCs present better capacitance behaviors than symmetric supercapacitors [39]. However, some other voices and arguments have emerged in view of the unsatisfactory capacitance properties certified by some recent anion adsorption/desorption experiments [40, 41]. On the one hand, some researchers stick to the view that the adsorption/desorption of  $\text{Zn}^{2+}$  on carbon-based composites contributes to the capacitance (Eq. (3)) [42, 43]. On the other hand, the capacitance is believed to be increased by the adsorption/desorption of anions on carbon-based hybrids (Eq. (4)) [44]. For

example, three different zinc cation electrolytes (zinc sulfate, zinc acetate, and zinc chloride) were applied to probe the influence of electrolyte anions on the electrochemical properties of zinc-ion hybrid capacitors, demonstrating the role of anions in electrochemical energy storage [45]. In summary, the future development of supercapacitors is injected with new energy in the emerging ZIHCs devices while brightening the route to achieving capacitors with better electrochemical properties. The complex energy storage principle of ZIHCs has been gradually established with constant explorations.

$$C = \frac{1}{\frac{1}{C_+} + \frac{1}{C_-}} \tag{2}$$



ZIHCs are electrochemical devices consisting of battery-type anodes and capacitor-type cathodes; hybrid structures consist of zinc-ion batteries and supercapacitors (Fig. 2) [46]. During the charging process, the anions in the electrolyte move and adsorb to the cathode (or are trapped in the cathode) in order to obtain an electric double layer (EDLC), while the Zn<sup>2+</sup> in the electrolyte moves and deposits on the zinc anodes. The discharge process is the opposite of the charging process, with the anions and Zn<sup>2+</sup> on the electrode diffusing back into the electrolyte. The cathode electrodes of ZIHCs always adopt the carbon-based structure with large porosity to accommodate the intercalation/extraction of ions, which are separated from the metallic zinc anodes

by a permeable insulating separator. And soluble zinc salt solutions are usually applied as electrolytes in ZIHCs due to the high stability, low viscosity, and high ion transport rate of Zn<sup>2+</sup> in aqueous solutions [47]. However, aqueous electrolytes always lead to a limited voltage range between 0.2 and 1.8 V based on the competitive decomposition of water. The non-aqueous electrolytes were reported to increase the voltage range to exceed 1.8 V but with problems of safety and economy [48]. In contrast, electrolyte improvement is a superior measure, which will be discussed in “Performance regulation of ZIHCs.”

### 3 Carbon-based electrode materials for ZIHCs

Carbon-based materials have been tremendously investigated as supercapacitor electrodes in terms of their high hole density, large specific surface area, outstanding conductivity, excellent stability, abundant raw materials, and safety [49–52]. In previous studies on ZIHCs, the charge storage capacity of carbon materials was demonstrated to be originated from the interface of the electrode/the electrolyte, and the electrochemical performance of ZIHCs was also influenced by the mentioned factors. Therefore, multitudinous carbon materials, including biomass carbon (BC), activated carbon (AC), heteroatom-doped carbon (HDC), and porous carbon (PC), are explored as electrodes for ZIHCs, and satisfactory performance was obtained. The recent works on ZIHCs consisting of carbon-based and Zn electrodes with ideal electrochemical properties are listed in Table 1, which illustrates their promising practical commercial application.

#### 3.1 Activated carbon material

Activated carbon materials have been widely investigated as potential electrode materials for ZIHCs, which exhibit excellent characteristics of large specific surface area, easily tunable porosity, low consumption, and high stability [65]. For instance, a zinc-ion hybrid capacitor consisting of commercial activated carbon (AC) as the cathode, metallic Zn as anodes, and Zn sulfate aqueous solution as the electrolyte was constructed by Dong et al. (Fig. 3a). The commercial AC displayed a large specific surface area of 1923 m<sup>2</sup> g<sup>-1</sup> due to its irregular surface particles and the rough morphology (Fig. 3b, c). The specially designed ZIHCs exhibited stable CV performance at scan rates of 2–1000 mv s<sup>-1</sup> (Fig. 3d, e), presented a capacitance of 121 mAh g<sup>-1</sup> and an energy density of 84 Wh kg<sup>-1</sup> at 0.1 A g<sup>-1</sup> (Fig. 3f, g), a high power output of 14.9 KW kg<sup>-1</sup>, and finally high capacity retention over 91% (Fig. 3i) that was achieved after 10,000 cycles [26]. For the sake of further investigating the effects

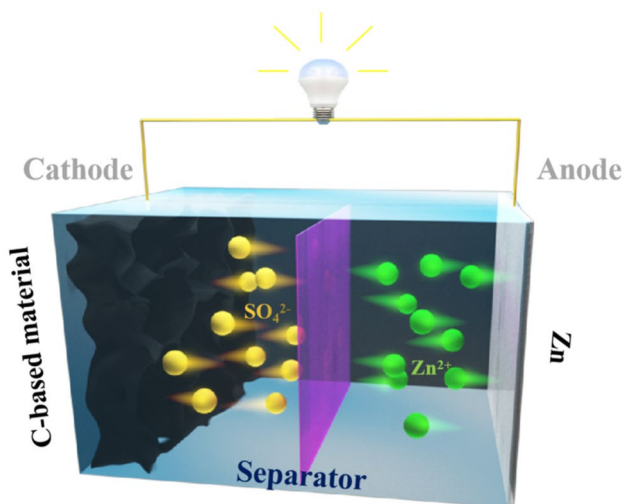


Fig. 2 Schematic representation of ZIHC composed of carbon-based cathodes and zinc anodes

**Table 1** Electrochemical characteristics summary of carbon-based materials in ZIHCs

Materials	Electrolyte	Voltage range (V)	Capacity	Current density (A g <sup>-1</sup> )	Electrochemical performance	Energy density (W h kg <sup>-1</sup> )	Power density (kW kg <sup>-1</sup> )	Ref.
AC	1 M Zn(CF <sub>3</sub> SO <sub>3</sub> ) <sub>2</sub>	0–1.7	170 F g <sup>-1</sup>	0.1	91% after 20,000 cycles	52.7	1.725	[53]
AC	2 M ZnSO <sub>4</sub>	0.2–1.8	121 mA h g <sup>-1</sup>	0.1	91% after 10,000 cycles	84	14.9	[26]
AC	2 M ZnSO <sub>4</sub>	0–1.8	72.1 mA h g <sup>-1</sup>	0.05	100% after 10,000 cycles	115.4 μWh cm <sup>-2</sup>	3.9 mW cm <sup>-2</sup>	[54]
CNT	1 M ZnSO <sub>4</sub>	0.2–1.8	83.2 mF cm <sup>-2</sup>	1 mA cm <sup>-2</sup>	87.4% after 6000 cycles	29.6 μWh cm <sup>-2</sup>	0.8 mW cm <sup>-2</sup>	[41]
PSC-A600	1 M Zn(CF <sub>3</sub> SO <sub>3</sub> ) <sub>2</sub>	0.2–1.8	183.7 mA h g <sup>-1</sup>	0.2	92.2% after 10,000 cycles	147	0.136	[44]
MSAC	2 M ZnSO <sub>4</sub>	0.3–1.8	176 mA h g <sup>-1</sup>	0.5	78% after 40,000 cycles	188	0.533	[55]
HPC	2 M ZnSO <sub>4</sub> @ 1 M Na <sub>2</sub> SO <sub>4</sub>	0.01–1.8	204 mA h g <sup>-1</sup>	0.2	94.9% after 2000 cycles	118	0.2	[56]
PCN	1 M ZnSO <sub>4</sub>	0.1–1.7	149 mA h g <sup>-1</sup>	0.2	91% after 10,000 cycles	119	0.16	[57]
PCNFs	1 M ZnSO <sub>4</sub>	0.1–1.7	177.7 mA h g <sup>-1</sup>	0.5	90% after 10,000 cycles	142.2	0.4	[58]
MPC	1 M Zn(CF <sub>3</sub> SO <sub>3</sub> ) <sub>2</sub>	0–1.8	209 F g <sup>-1</sup>	0.2	100% after 10,000 cycles	92.7	0.179	[59]
HCSs	2 M ZnSO <sub>4</sub>	0.15–1.95	86.8 mA h g <sup>-1</sup>	0.5	98% after 15,000 cycles	59.7	0.448	[60]
B/N co-doped LDC	1 M ZnSO <sub>4</sub>	0.2–1.8	127.7 mA h g <sup>-1</sup>	0.5	/	97.6	12.1	[40]
P@B-AC	2 M ZnSO <sub>4</sub>	0.2–1.8	169.4 mA h g <sup>-1</sup>	0.5	88% after 30,000 cycles	169.4	20	[61]
N-HPC	2 M ZnSO <sub>4</sub>	0.2–1.8	136.8 mA h g <sup>-1</sup>	0.5	90.9% after 5000 cycles	191	3.633	[62]
B-diamond/carbon fiber	1 M ZnSO <sub>4</sub>	0.2–1.8	35.1 F g <sup>-1</sup>	0.2	89.9% after 10,000 cycles	70.7	0.709	[63]
N-PC	2 M ZnSO <sub>4</sub>	0.15–1.7	302 mA h g <sup>-1</sup>	1.0	> 100% after 10,000 cycles	157.6	0.69	[64]

of specific surface area on AC electrodes for ZIHCs, a high-performance ZIHC was assembled by a three-dimensional porous AC material prepared by an organic salt precursor as the cathode with a high specific surface area of 2854.1 m<sup>2</sup> g<sup>-1</sup> and a rich micro/ultra-microporous structure, which exhibited a capacitance of 213 mAh g<sup>-1</sup>, energy density of 164 Wh kg<sup>-1</sup> and the power density of 390 W kg<sup>-1</sup> at t 0.5 A g<sup>-1</sup>, and high capacity retention of 90% after 20,000 cycles at 10.0 A g<sup>-1</sup> [66].

In short, the application of activated carbon materials ZIHCs is an innovative attempt and breakthrough; the feasibility of carbon materials on ZIHCs has been demonstrated based on the successful experimental results, which will lead the way for the subsequent application of other carbon material electrodes in ZIHCs.

### 3.2 Biomass-derived carbon material

Recently, the reuse value of various raw material-rich and renewable biomass wastes has been favored by researchers [67]. Biomass-derived carbon (BC) materials have the advantages of large specific surface area, tunable microstructure, and surface functional groups, which gradually become the most promising candidate materials for electrodes under the promotion of the two-carbon policy. For example, biomass-derived carbon stem from coconut shells was synthesized with a specific surface area of 3554 m<sup>2</sup> g<sup>-1</sup> and was applied as electrodes for ZIHCs (Fig. 4a–c), which presented a capacity of 170 F g<sup>-1</sup> at 0.1 A g<sup>-1</sup> (Fig. 4d–f) and an energy density of 52.7 Wh kg<sup>-1</sup> at 1725 W kg<sup>-1</sup> that calculated based on the active substance. Besides, the capacity retention can be up to

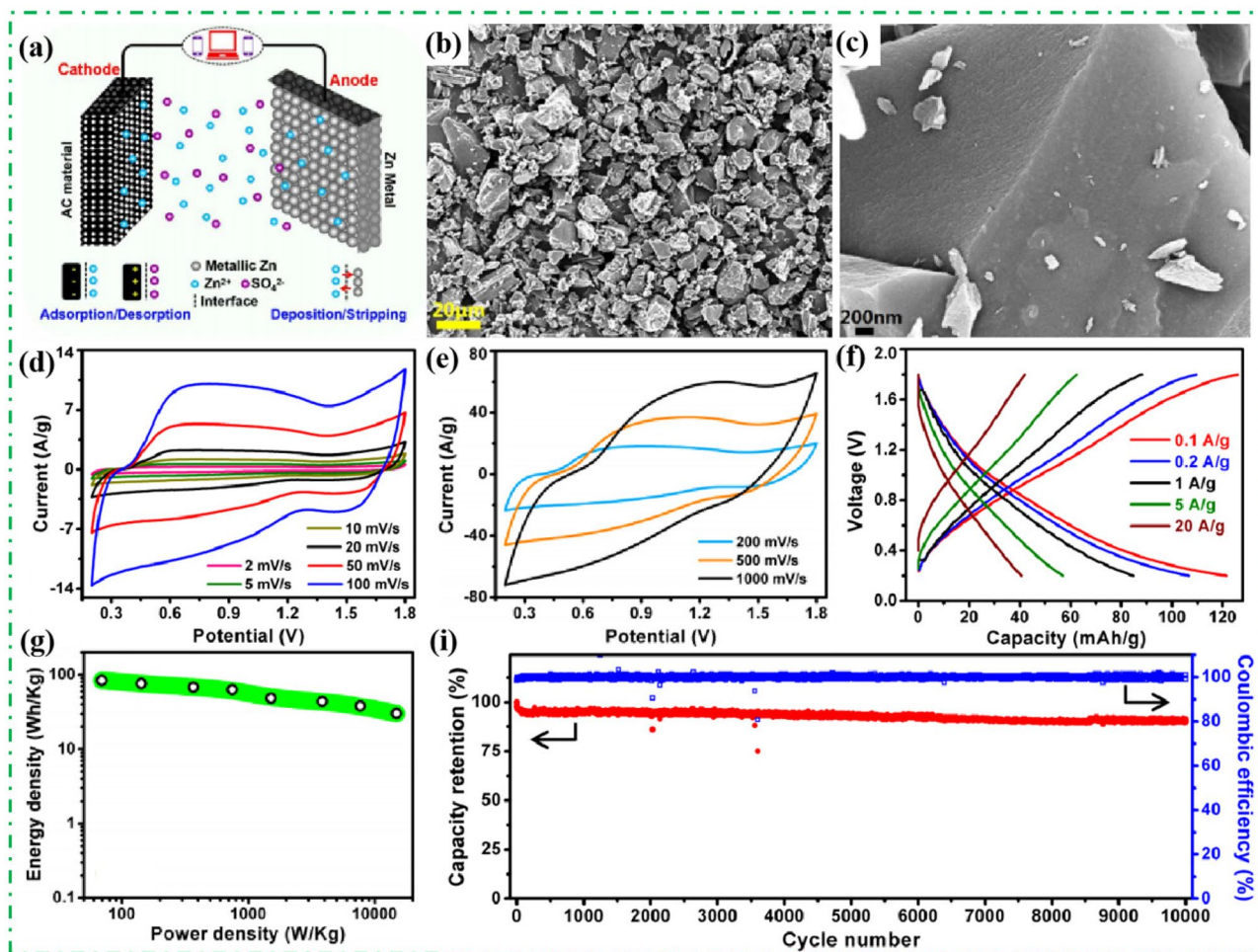


**Fig. 3** Morphology and electrochemical properties of AC: **a** schematic of AC//ZnSO<sub>4</sub> (aq)//Zn system; **b**, **c** SEM images of AC powder; **d**, **e** CV curves at 2.0–1000 mV s<sup>-1</sup>; **f** GCD curves at 0.1–20 A g<sup>-1</sup>; **g** Ragone plot; **h** cycling performance at 1.0 A g<sup>-1</sup> of ZIHCS. Reproduced with permission from [26]. Copyright 2018, Elsevier

nearly 100% after 22,000 lifespans at 1.0 A g<sup>-1</sup> (Fig. 4g) and over 91% after 20,000 cycles even at 2.0 A g<sup>-1</sup> (Fig. 4h) [53]. Meanwhile, corncob-derived carbon materials were prepared by single-step calcination of the low-cost corncob wastes, which were applied as cathode electrodes for ZIHC (Fig. 5a). The specific surface area of active corncob-derived carbon (ACC) materials reached up to 2619 m<sup>2</sup> g<sup>-1</sup> after the single-step carbonization and activation (Fig. 5b,c) and exhibited exceptional specific capacitance in an alkaline electrolyte (Fig. 5d), acidic electrolyte (Fig. 5e), and neutral electrolyte (Fig. 5f). Simultaneously, the GCD curves of the ZIHC presented the typical linear shapes (Fig. 5g), an energy density of 94 Wh kg<sup>-1</sup> at 68 W kg<sup>-1</sup> (Fig. 5h), and good cycling stability of high capacity retention over 98.2% after 10,000 lifespans at 5.0 A g<sup>-1</sup> (Fig. 5i) [68]. Furthermore, a high mesoporous carbon material originating from agricultural waste corn silk

was prepared and showed excellent energy storage performance for both supercapacitor and ZIHCS. The assembled supercapacitor delivered an energy density of 25 Wh kg<sup>-1</sup> and a remarkable cycling lifespan at a high power density of 23,070 W kg<sup>-1</sup>; in contrast, a high energy density of 38.5 Wh kg<sup>-1</sup> at the high power density of 14,741 W kg<sup>-1</sup> for the ZIHC was achieved. The results not only demonstrated the feasibility of mesoporous carbon materials as electrode materials for supercapacitors and ZIHCS but also reflected the superior electrochemical performance of ZIHCS compared with supercapacitors [69].

Compared with activated carbon, biomass-derived carbon materials present the advantages of an abundant resource and adjustable surface chemical information and are beneficial to the sustainable utilization of resources and the establishment of an environment-friendly society.

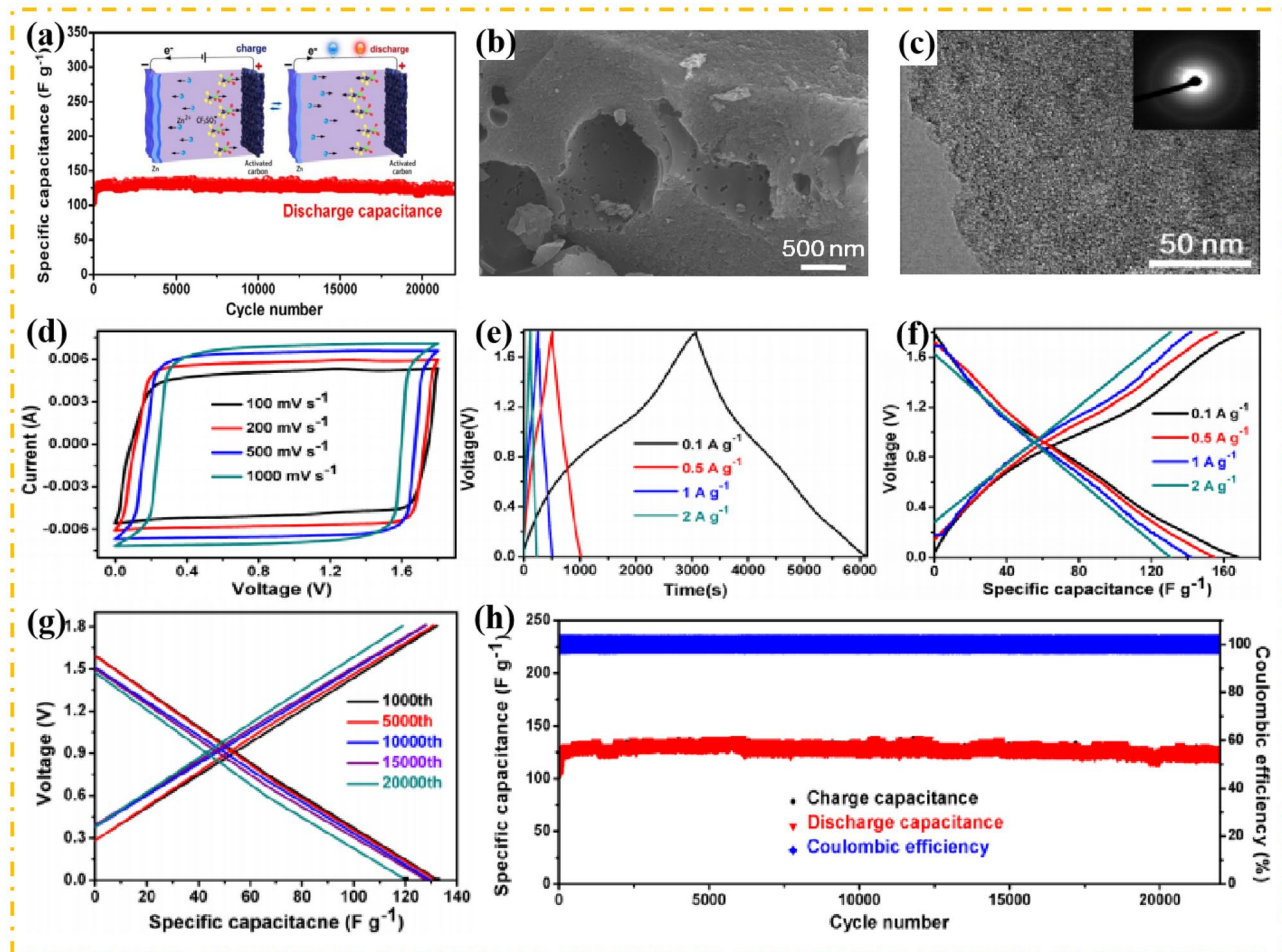


**Fig. 4** Morphology and electrochemical properties of BC derived from coconut shells: **a** schematic diagram of ZIHC working principle and cycle performance. **b** SEM and **c** TEM image of coconut shell. **d** CV curves of ZIHC at 100–1000  $\text{mV s}^{-1}$ . **e** GCD curves of ZIHC at 0.1–

2.0  $\text{A g}^{-1}$ . **f** Voltage-specific capacitance curves of ZIHC at 0.1–2.0  $\text{A g}^{-1}$ . **g** GCD curves of the ZIHC after 1000–20,000 cycles. **h** Cycling property of the ZIHC at 2.0  $\text{A g}^{-1}$ . Reproduced with permission from [53], Copyright 2017, Elsevier

### 3.3 Porous carbon material

The significant characteristic of porous carbon materials roots in the abundant pore structure that enables the regulation of specific surface area. In addition, the advantages of abundant raw materials and easy regulation promote the wide explorations of porous carbon acting as cathode electrodes for ZIHCs [70]. Two-dimensional porous carbon nanoflates (PCNF) were synthesized via chemical etching technique using sodium polyacrylate powder mixed with potassium bicarbonate powder [58]; the preparation routes are shown in Fig. 6a. The as-prepared PCNF presents submitted a stacked nanosheet-like structure (Fig. 6b), and the pore structure is identified by the HRTEM image (Fig. 6c); the specific surface area of PCNF-4 is as high as 1770  $\text{m}^2/\text{g}$ , which presented satisfactory capacity retention over 90% after 10,000 lifespans at 10.0  $\text{A g}^{-1}$  (Fig. 6d). The ZIHC assembled with PCNF as cathode achieved an

energy density of 142.2  $\text{Wh kg}^{-1}$  at a power density of 400.3  $\text{W kg}^{-1}$  at 0.5  $\text{A g}^{-1}$ , an energy density of 68.4  $\text{Wh kg}^{-1}$  even at the power density of 15,390  $\text{W kg}^{-1}$  at 20  $\text{A g}^{-1}$  (Fig. 6e), which demonstrated the excellent energy output capability of ZIHCs. Furthermore, two green diodes were lighted by the assembled ZIHCs, which demonstrate their potential application (Fig. 6f). Meanwhile, a graded porous carbon (PSC) stem from pencil shavings with hierarchical porous structure and high specific surface area of 1293  $\text{m}^2/\text{g}$  was prepared (Fig. 7a) [43]. The ZIHC consisted of PSCs as positive and metallic Zn as negative electrode companied with  $\text{Zn}(\text{CF}_3\text{SO}_3)_2$  solution as electrolyte exhibited superior rate capability and ultra-high exceptional capacity of 183.7  $\text{mA g}^{-1}$  (Fig. 7b–d), a maximum energy of 147.0  $\text{kWh kg}^{-1}$ , a maximum power density of 15.7  $\text{kW kg}^{-1}$  (Fig. 7e), and an impressive 92.2% capacitance retention after 10,000 lifespans at 10.0  $\text{A g}^{-1}$  (Fig. 7f). More surprisingly, the ZIHC maintained

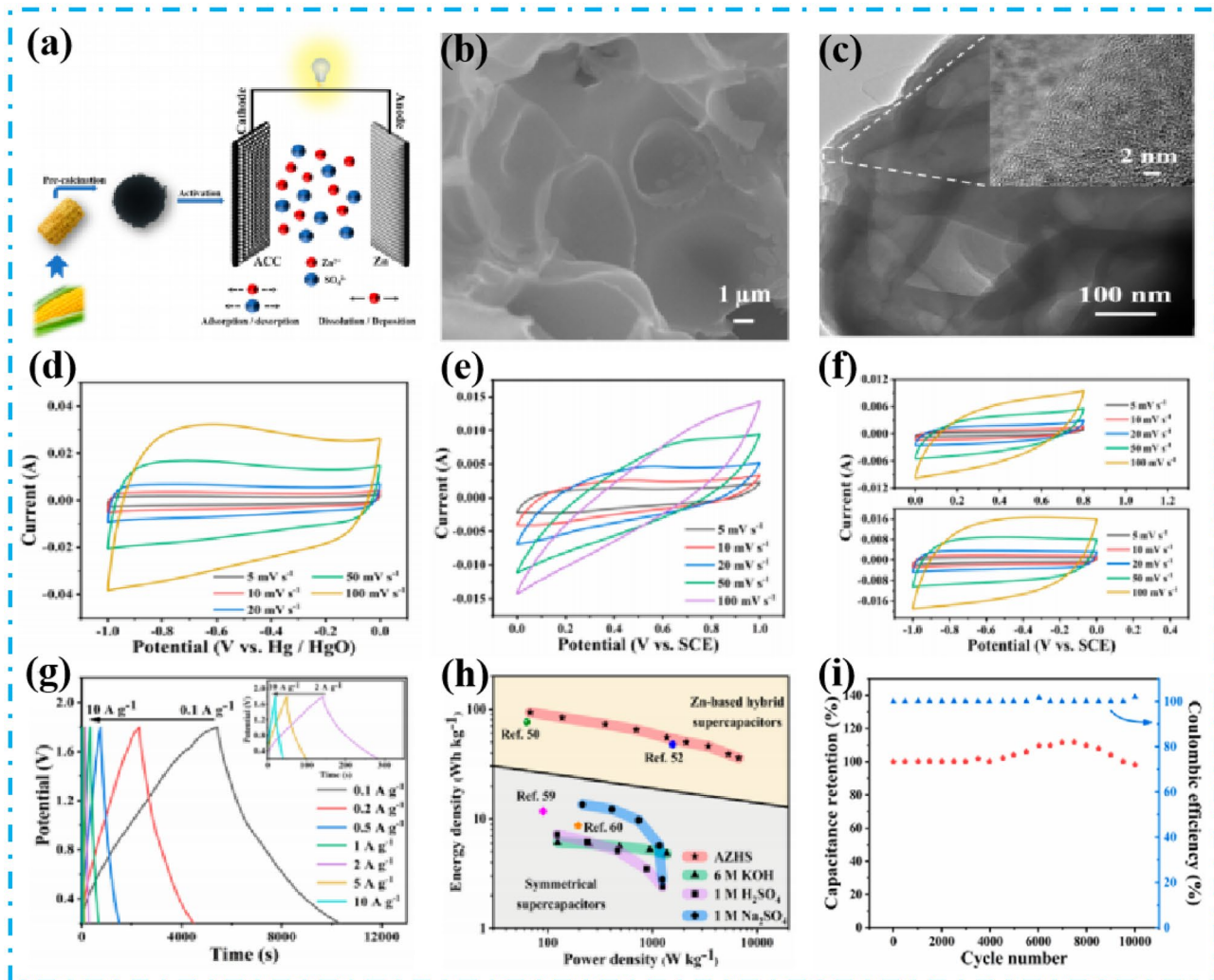


**Fig. 5** **a** Diagrammatic sketch of corn cob applied as an electrode for ZIHC. **b** SEM image and **c** TEM image of ACC. Three-electrode electrochemical performance of ACC samples in **d** KOH electrolytes, **e** H<sub>2</sub>SO<sub>4</sub> electrolytes, and **f** Na<sub>2</sub>SO<sub>4</sub> electrolytes. **g** GCD curves of

ZIHC at 0.1–10.0 A g<sup>-1</sup>. **h** Ragone plots of ZIHC and some supercapacitors reported in the literature. **i** Cycling performance of ZIHC at 5 A g<sup>-1</sup>. Reproduced with permission from [68], Copyright 2019, ACS

excellent antifreeze performance (nearly 100% coulombic efficiency at -15 °C) and cycling stability (over 80 cycles) when antifreeze hydrogel is added to the electrolyte system (Fig. 7g). Besides, a 3D hierarchical porous carbon (3D HPC) derived from waste bagasse, and coconut shells was obtained by process of hydrothermal carbonization and potassium hydroxide activation (Fig. 8a) [56]; the strong porosity gives HPC a high surface area of 3401 m<sup>2</sup> g<sup>-1</sup> and a large pore volume of 2.03 cm<sup>3</sup> g<sup>-1</sup>. The porous structure (Fig. 8b–d) endows it with good electronic conductivity, resulting in excellent electrochemical performance when assembled into ZIHCS as a cathode. ZIHCS exhibit a capacitance of 305 mAh g<sup>-1</sup> at 0.1 A g<sup>-1</sup> (Fig. 8e), a high energy density of 118 Wh kg<sup>-1</sup>, outstanding rate performance, and remarkable cycling stability with a capacitance

retention rate of 94.9% after 20,000 cycles at 2.0 A g<sup>-1</sup> (Fig. 8f).

The porous carbon materials endowed with excellent adsorption properties are believed to be one of the most promising and popular carbon-based composites in the future. The rational synthesis of porous carbon materials through the targeted design of reaction routes, surface modification, etc. is of outstanding significance for enhancing the capacity of ZIHCS.

### 3.4 Heteroatom-doped carbon

Compared with pure carbon materials, the introduction of heteroatoms into the carbon matrix is regarded as an effective way to enhance their electrochemical properties. Among

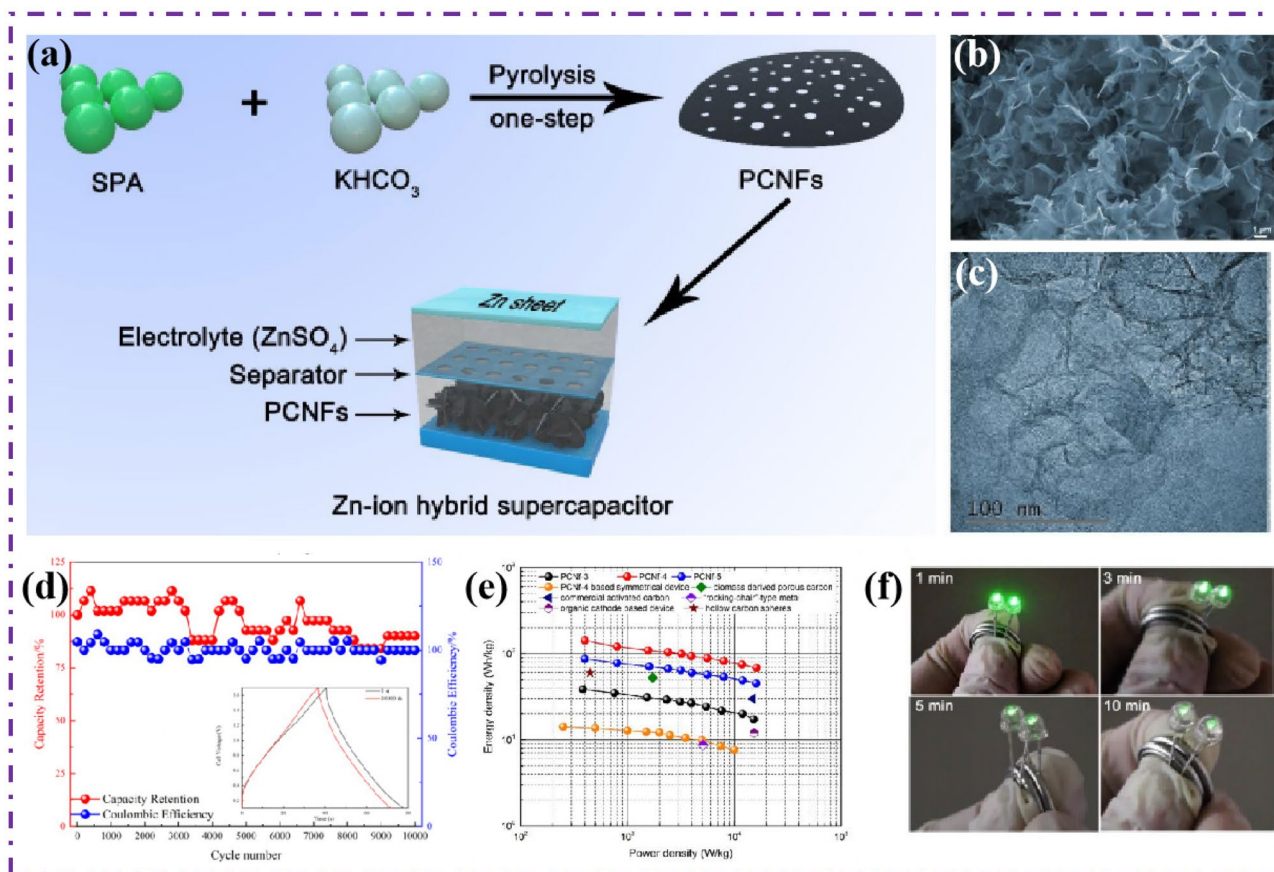


**Fig. 6** Morphology and electrochemical properties of PCNF: **a** schematic diagram of the synthesis process and energy storage application of PCNFs. **(b)** FESEM images of PCNF-4. **(c)** TEM images of PCNF-4. **(d)** Cycling performance of ZIHC at  $10 \text{ A g}^{-1}$  (insert is the GCD curves). **(e)** Ragone plots of PCNFs-based ZIHCs, PCNF-4-based sym-

metric supercapacitors, and other previously reported ZIHCs. **(f)** Photograph of two PCNF-4-based ZIHCs lit up with two green LEDs after charging for 60 s at  $5 \text{ A g}^{-1}$ . Reproduced with permission from [58], Copyright 2020, Elsevier

various heteroatoms, nitrogen atom with large electronegativity contributes to the improvement of electronic conductivity and active site numbers, promoting the increase of capacitance, rate capability, and cycling stability, which is the most widely investigated and promising heteroatom dopant [71]. For example, an aqueous ZIHC consisting of a layered N-doped carbon cathode and metallic Zn anode with high energy and cycling stability was proposed [72]. The ZIHC devices exhibited a high energy density of  $107.3 \text{ Wh kg}^{-1}$ , an excellent power density of  $24.9 \text{ kW kg}^{-1}$ , and satisfactory capacity retention beyond 99.7% after 20,000 cycles at  $4.2 \text{ A g}^{-1}$ , which proved the chemisorption process of  $\text{Zn}^+$ , surface wettability, and conductivity of the electrode material are enhanced by the introduced nitrogen heteroatoms. In addition, a nitrogen and oxygen co-doped-layered HPC/CC synthesized by drop coating and carbonization was reported by Zhao et al. (Fig. 9a) [73]. The uniquely designed composites with plentiful nitrogen and oxygen dopants also presented large pore volumes due to the layered pore construction of micro- and middle holes (Fig. 9b)

and exhibited excellent electrochemical behaviors as ZIHC cathodes, including a high capacity of  $138.5 \text{ mAh g}^{-1}$  at  $0.5 \text{ A g}^{-1}$ , superior rate capability at  $20.0 \text{ A g}^{-1}$ , and superior  $\text{Zn}^+$  storage performance (Fig. 9c). Most notably, the original capacity increased to 104.3% after 10,000 cycles because the pores were slowly penetrated by electrolyte ions during cycling (Fig. 9d).

Besides nitrogen and oxygen heteroatoms, other heteroatoms can be applied to dope into the carbon matrix to enhance the storage behaviors of  $\text{Zn}^+$ . For instance, the wettability of electrolyte/electrode can be improved by doping phosphorus elements. Meanwhile, more structural defects would be generated due to the different van der Waals radii of phosphorus (195 pm) and carbon (180 pm). The boron elements present a similar van der Waals radius and valence electron number of carbon, which hardly affects the lattice parameters of carbon but can improve the electronic conductivity [74]. A boron and phosphorus co-doped-activated carbon material (P, B-AC) was achieved by a one-step doping calcination method (Fig. 10a–c), which displayed a high



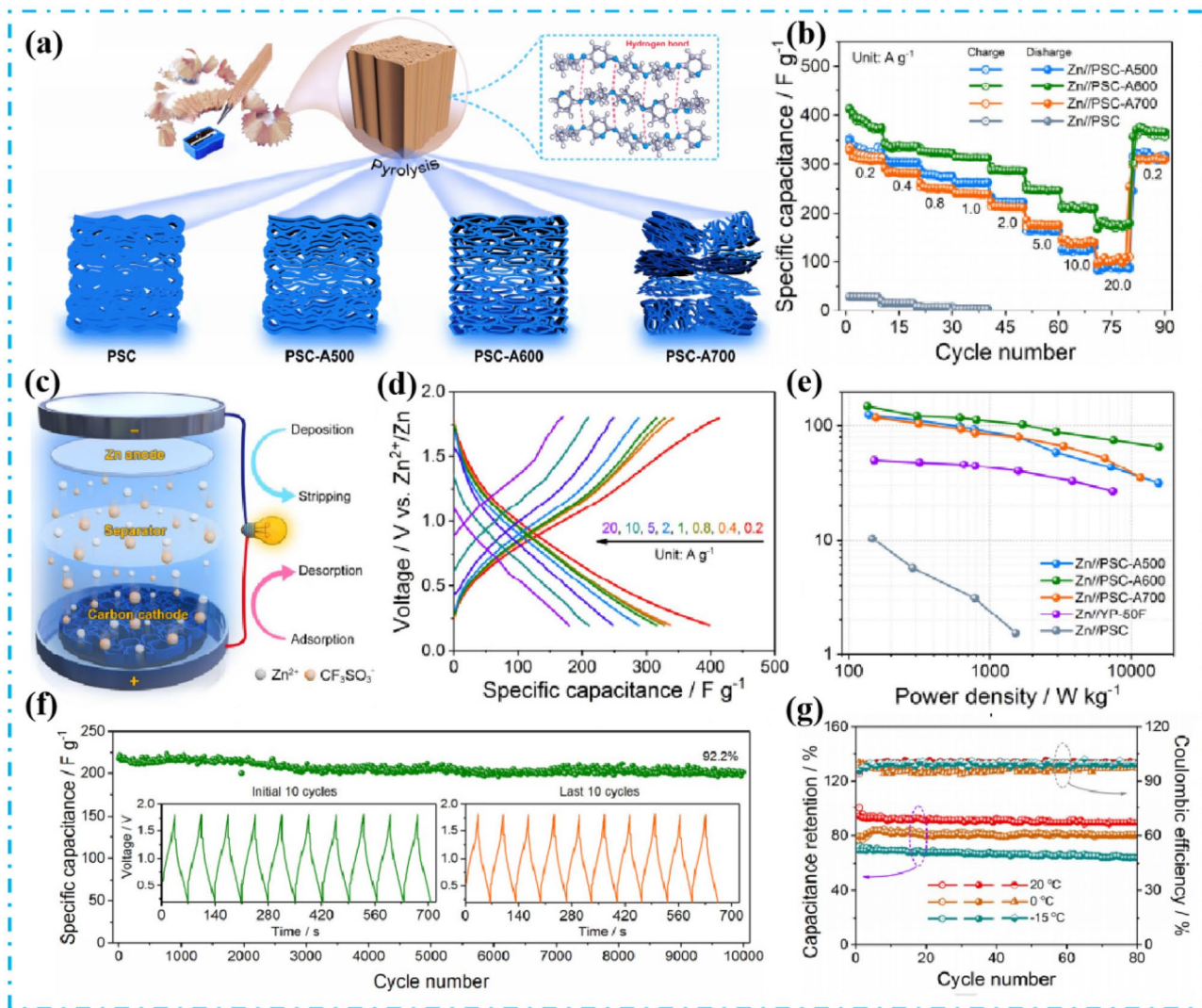


**Fig. 7** Morphology and electrochemical properties of PSC: **a** schematic diagram of PSCs. **b** Rate capability of PSCs. **c** Schematic diagram of the structure of ZIHC. **d** GCD profiles of the PSC-A600 at 0.2~20.0 A g<sup>-1</sup>. **e** Ragone plots of PSCs. **f** Cycle graph over 10,000

times (insert is the first and last 10 GCD curves). **g** Capacity retention at low temperatures. Reproduced with permission from [44], Copyright 2020, Elsevier

capacitance of 169.4 mAh g<sup>-1</sup> at 0.5 A g<sup>-1</sup> (Fig. 10d, e), superior ion mobility (Fig. 10f), and an energy density of 169.4 Wh kg<sup>-1</sup> and exhibited an excellent power density of 500 W kg<sup>-1</sup> and capacity retention over 88% after 30,000 cycles (Fig. 10g).

In general, it is a promising strategy to construct carbon matrix cathodes for high-performance ZIHCs by introducing various heteroatoms in terms of their distinctive electronic structures and properties. However, precisely tuning the morphological structure of the doping and achieving stable reproducibility is still a big challenge. Furthermore, the mechanism of action of the synergistic effect of different heteroatom doping is also one of the directions that need to be further explored.

In short, carbon-based materials are generally characterized by a large surface area to allow fast and easy access to the electrode surface, absorbing electrolyte ions to the surface of the electrode material and thus improving the electrochemical performance.

Although enormous research has been focused on zinc ion supercapacitor carbon-based material electrodes, their practical applications are still limited, and advanced carbon-based electrodes are still in great demand.

### 4 Performance regulation of ZIHCs

The short circuits and cell failure of ZIHCs would occur due to the puncture of the electrolyte diaphragm caused by the formation and growth of zinc dendrite. Furthermore, more

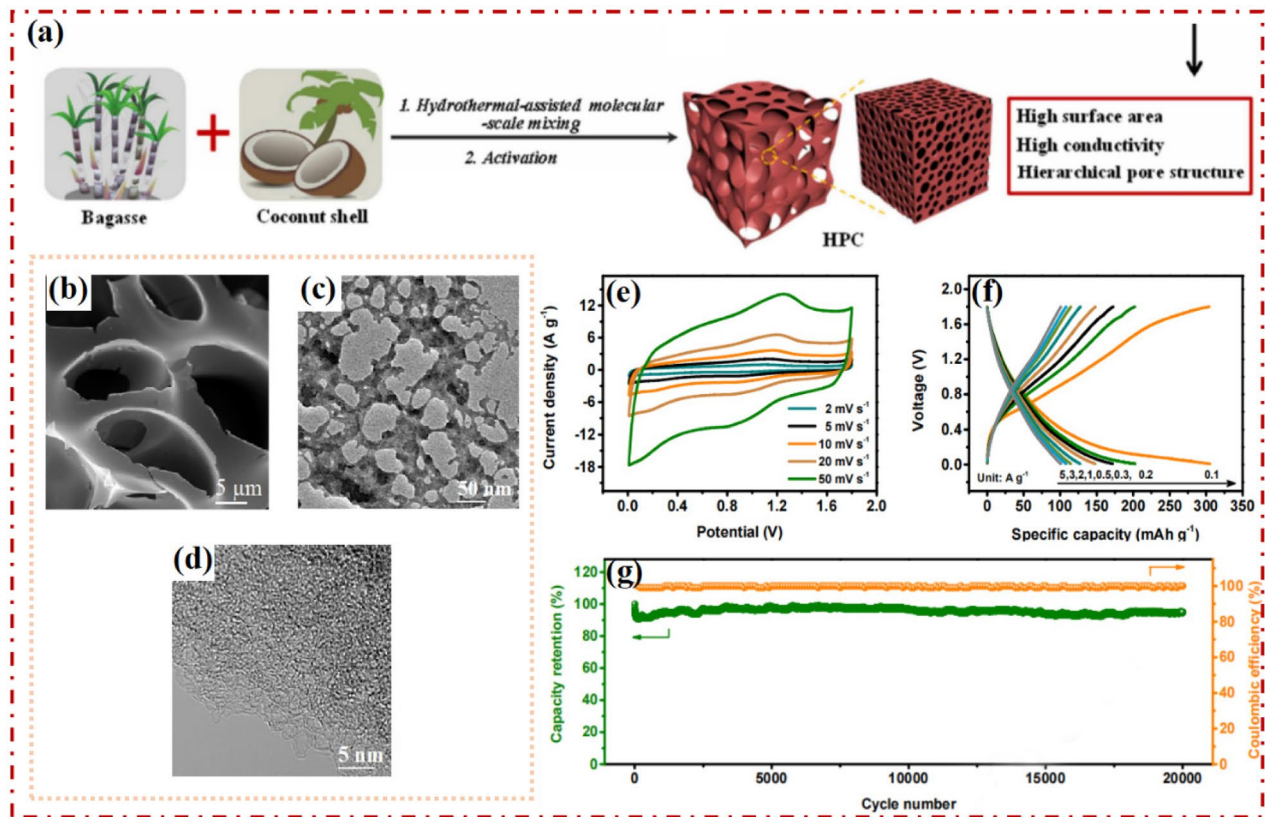


**Fig. 8** Morphology and electrochemical properties of HPC: **a** schematic diagram of HPC. **b** SEM image, **c** TEM image, and **d** HRTEM of HPC. **e** CV curves of HPC-based ZIHC at 2.0–50.0  $\text{mV s}^{-1}$ .

**f** GCD profiles of HPC-based ZIHC at 0.1–5.0  $\text{A g}^{-1}$ . **g** Cycling stability at 2.0  $\text{A g}^{-1}$  over 20,000 cycles of HPC-based ZIHC. Reproduced with permission from [56], Copyright 2019, Elsevier

severe dendrite occurs in alkaline electrolytes compared with neutral or essential electrolytes, which may be attributed to the  $\text{Zn}(\text{OH})_4^{2-}$  produced by oxidation or self-corrosion at Zn anode in alkaline electrolytes [75]. The formed  $\text{Zn}(\text{OH})_4^{2-}$  unevenly distributes on the surface of the zinc electrodes and accumulates gradually and prominently, and uneven Zn negative surface current accelerates the formation of Zinc dendrites, leading to the failure of electrochemical behaviors [76]. The obvious one-dimensional (1D) zinc dendrites are always observed even at low current densities in alkaline electrolytes, but hardly observed at low current densities in neutral and acidic electrolytes [77], which promote the more widespread application of acid or neutral electrolytes for ZIHCs. Nevertheless, obtaining ZIHCs with desirable cycling performance in acid/neutral electrolytes is challenging because numerous large-sized dendrites are still generated, aggregated, and nucleated on the Zn anode at high current densities, causing the performance paralysis of the capacitor devices. Consequently, electrode surface modification and the introduction of additives into electrolytes are effective strategies to alleviate the formation of zinc dendrites and improve the electrochemical performance of ZIHCs, which are becoming one of the focuses in the further exploration of ZIHCs.

#### 4.1 Improving the negative electrodes

Currently, the introduction of coatings on the surface of Zn electrode and/or designing unique structured zinc anodes are regarded to be the most direct, effective, and extensive research strategies for restraining the formation and growth of zinc dendrite [78–81]. An effective coating should meet the requirements of electrochemical compatibility with the zinc electrode and electrolytes and excellent mechanical strength to suppress the growth of zinc dendrites.

Carbon and polymer-based coatings are always chosen for zinc anode protection [82]. For example, the Zn electrodes covered by carbon nanotubes (CNTs) were built [83], where the porous framework can mechanically adjust the volume change and offer a stable electric field during Zn desorption/deposition, hindering the formation and growth of Zinc dendrites and the occurrence of side reactions. With the protection of carbon-based coating, the Zn anode with a stable scaffold exhibited high chemical stability and excellent reversibility, leading to the enhanced ultralong stable cycling lifespan of ZIHC (over 1800 h). Besides carbon-based coating, polymer-based coating with an elastic layer is beneficial to alleviate shape mutation and induce the lateral deposition

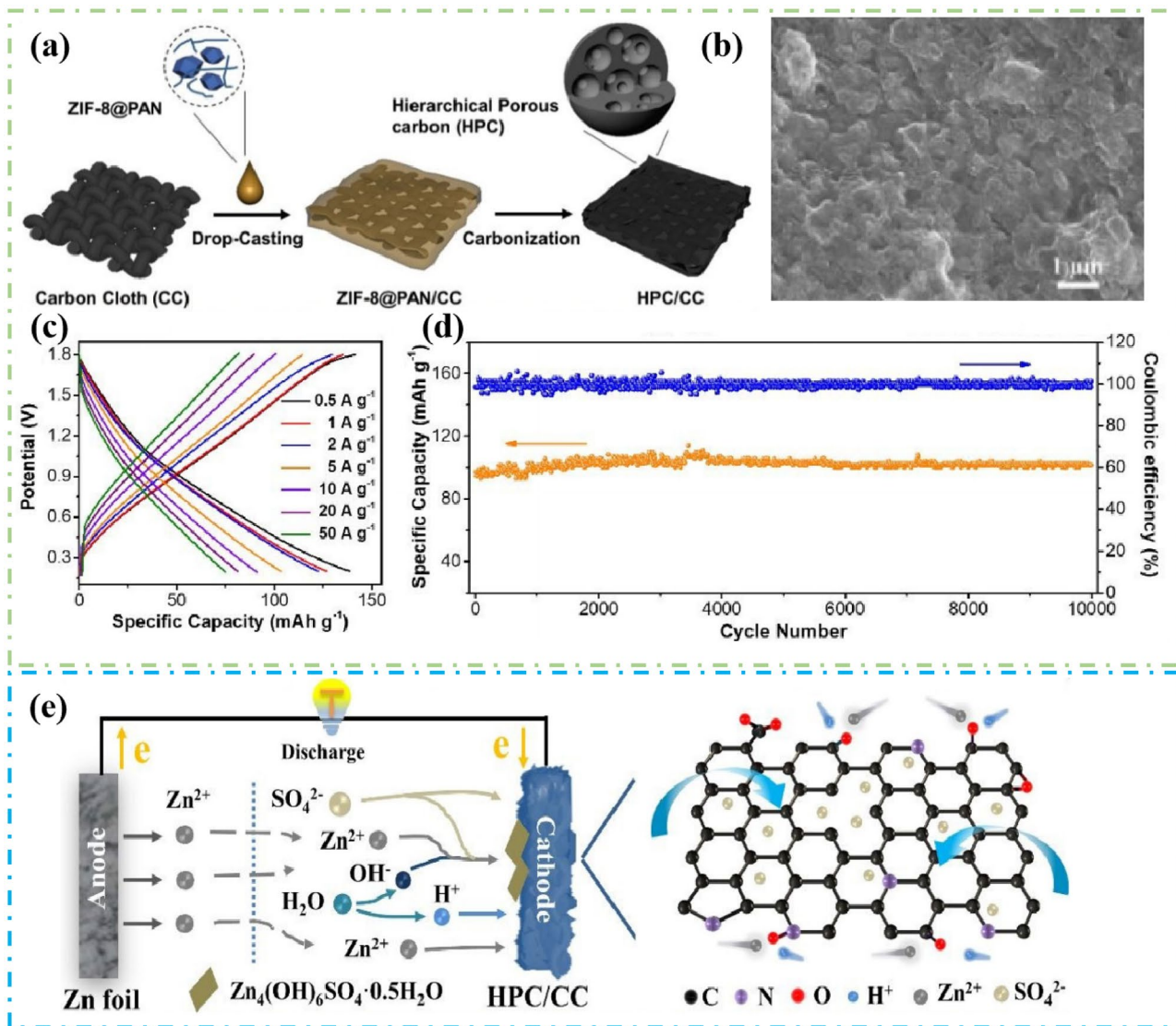


**Fig. 9** Morphology and electrochemical properties of HPC/CC: **a** diagrammatic sketch of HPC/CC synthesis; **b** SEM image of HPC/CC; **c** GCD curves of HPC/CC-based ZIHC at 0.5–50.0 A g<sup>-1</sup>; **d** cycling

stability of HPC/CC-based ZIHC at 5 A g<sup>-1</sup>; **e** schematic diagram of ZIHC assembled with HPC/CC. Reproduced with permission from [73], Copyright 2019, RSC

of zinc dendrites [84]. The polyamide films were covered on zinc electrode surfaces by Zhao et al. [85], where the side reactions of zinc ions when passing through the polyamide membrane can be effectively suppressed, thanks to the desolvation of hydrated zinc ions by the polyamide membrane, resulting in satisfactory electrochemical performance. Furthermore, the unique prepared coating limits the diffusion of Zn<sup>2+</sup> and tunes the deposition process of Zn electrodes due to the coordination of amide groups with Zn<sup>2+</sup>.

The dominant factor that should be considered in material selection is the affinity with the zinc electrodes when adopting a coating protection strategy. The coating materials with a good affinity for zinc electrodes could effectively tune the electric field, reduce overpotentials, and enhance

the uniform deposition on the surface of Zinc, resulting in the enhanced cycling performance of ZIHCs.

### 4.2 Electrolyte regulation

Electrolyte additives can endow Zn<sup>2+</sup> diffuse and deposit more uniformly and inhibit side reactions, hindering the formation and growth of zinc dendrites, which have attracted enormous attention in improving the performance of ZIHCs. For example, a superior electrochemical performance ZIHC with multi-valent metal ion electrolyte by adding 0.1 M MgSO<sub>4</sub> in 2.0 M ZnSO<sub>4</sub> electrolyte was reported (Fig. 11a) [86]. The results that proved the multi-advantages of the introduction of Mg<sup>2+</sup> into the electrolyte were obtained. First, the formation and growth

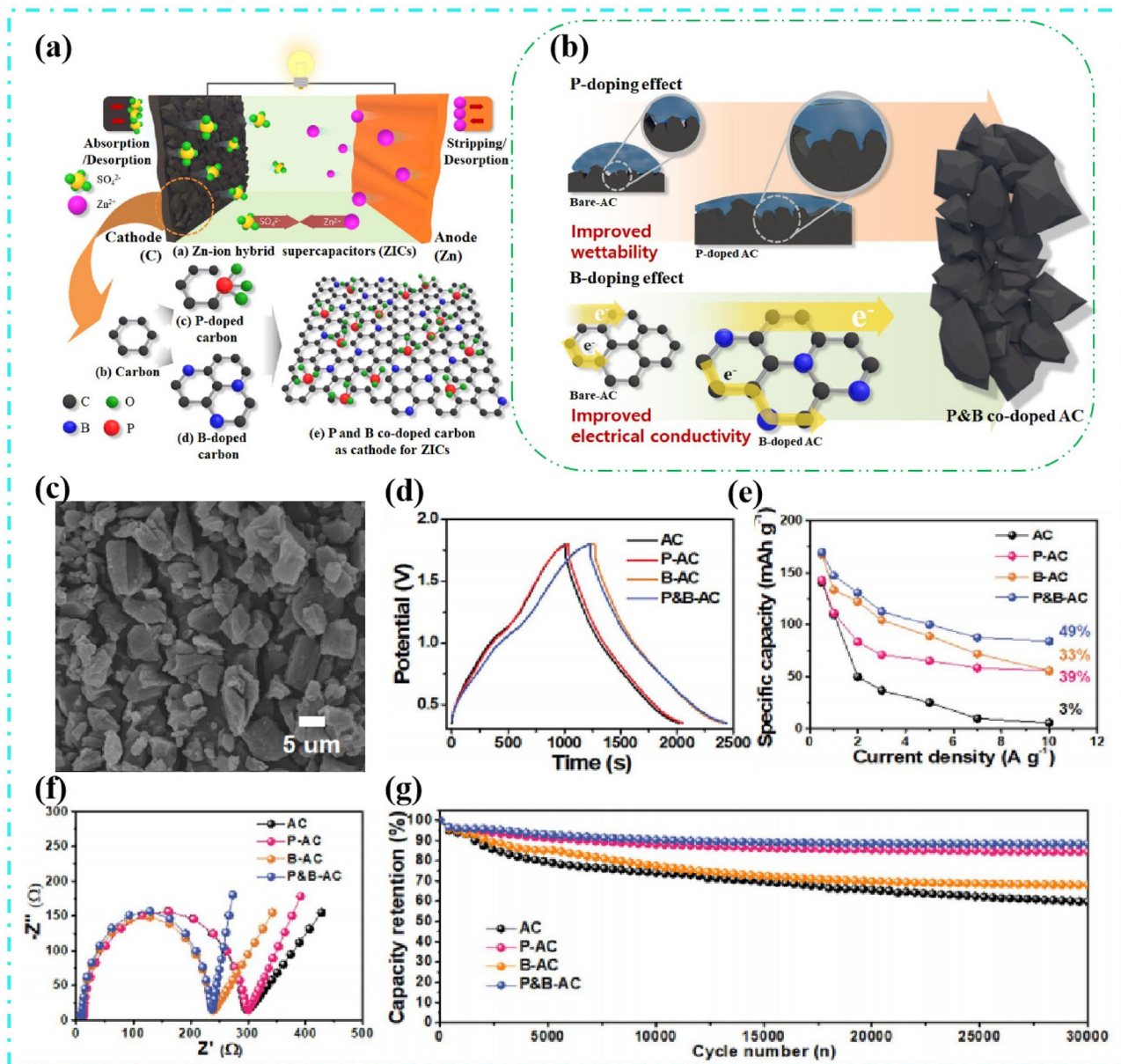


**Fig. 10** Morphology and electrochemical properties of P&B-AC and other comparative samples: **a** schematic diagram of ZIHC with P&B-AC as a positive electrode; **b** schematic diagram of the advantages of the optimized P&B-AC performance; **c** SEM image of P&B-AC;

**d** GCD curves at  $0.5 \text{ A g}^{-1}$ ; **e** specific capacity under different current densities; **f** Nyquist plots; **g** longevity performance for up to 30,000 cycles at  $10.0 \text{ A g}^{-1}$ . Reproduced with permission from [55], Copyright 2020, ACS

of zinc dendrites on the Zn electrode surface are effectively inhibited, and the side reactions of ion exchange between the Zn anode and electrolyte are weakened (Fig. 11b–e). The ZIHCs with Zn-Mg mixed electrolyte exhibited electrochemical behaviors, including a high capacitance of  $154 \text{ mAh g}^{-1}$  at  $1.0 \text{ A g}^{-1}$  (Fig. 11f) and high capacity retention over 98.7% after 10,000 cycles at  $5.0 \text{ A g}^{-1}$  (Fig. 11g). Mai et al. [87] proposed a high-performance ZIHC (ACC//Zn ZIHC) consisting of activated carbon coat as cathode, metallic Zn as anode, and  $\text{ZnSO}_4/\text{Na}_2\text{SO}_4$  solution as electrolyte. The experiment

results illustrated that the Zn anode was protected, and the capacitive storage of the ACC cathode was improved due to the intermediate  $\text{Zn}_4\text{SO}_4(\text{OH})_6 \cdot 0.5\text{H}_2\text{O}$  that was suppressed by adding  $1.0 \text{ M Na}_2\text{SO}_4$  into  $1.0 \text{ M ZnSO}_4$  electrolyte. Besides, the voltage window was broadened to  $1.9 \text{ V}$ , and the energy densities of  $100 \text{ Wh kg}^{-1}$  and  $20 \text{ Wh kg}^{-1}$  at power densities of  $50.42 \text{ W kg}^{-1}$  and  $1692 \text{ W kg}^{-1}$ , respectively, were achieved in this ZIHCs system.

In addition to cationic electrolyte additives, anionic electrolyte additives have also been identified to effectively improve

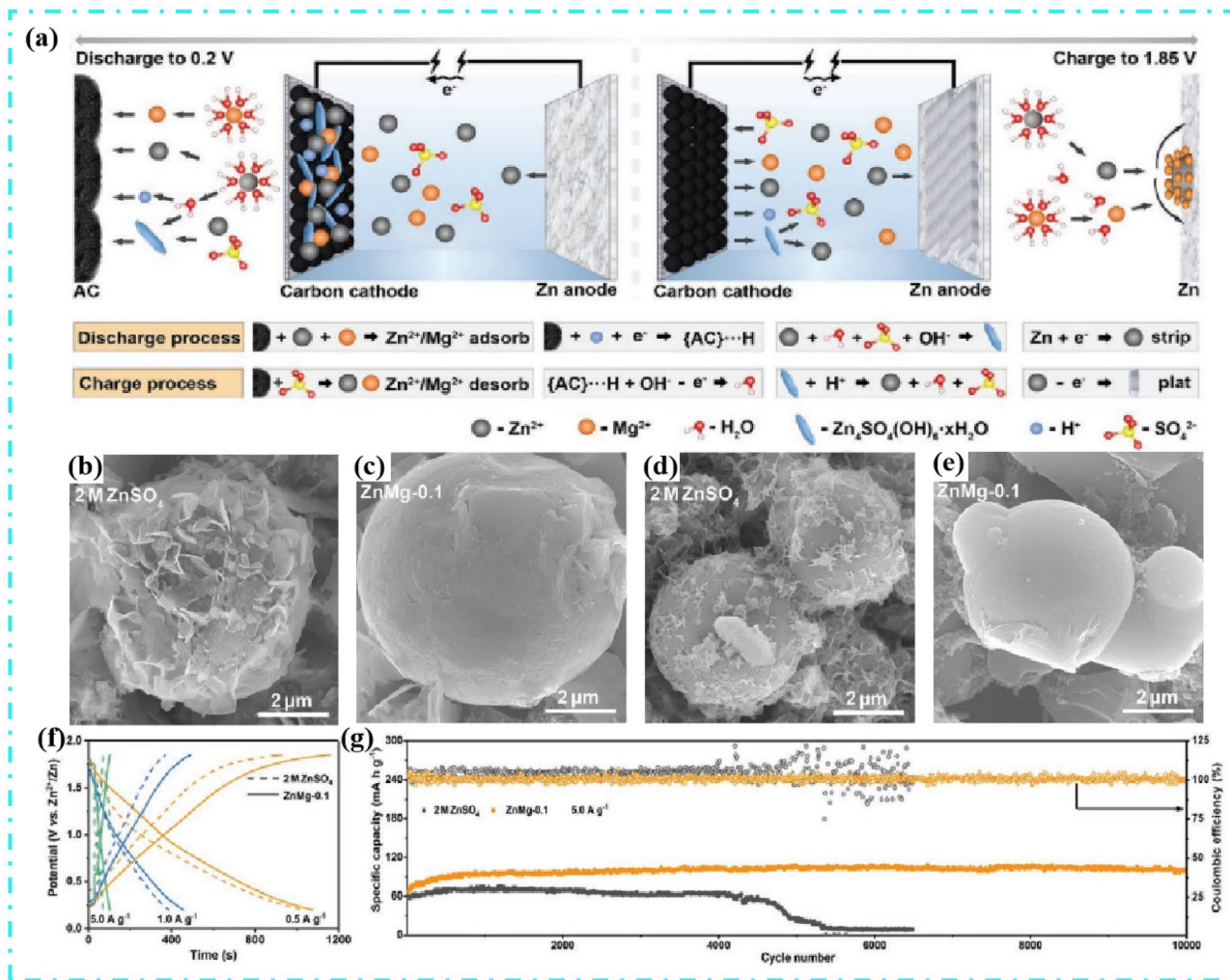


**Fig. 11** Morphology and electrochemical properties of AC: **a** schematic diagram of the structure of AC//ZnMg-0.1//Zn equipment and its mechanism of action; **b** SEM image of AC in ZnSO<sub>4</sub> electrolyte (discharge state); **c** SEM image of AC in ZnMg-0.1 electrolyte (discharge state); **d** SEM image of AC in ZnSO<sub>4</sub> electrolyte (charge state); **e** SEM

image of AC in ZnMg-0.1 electrolyte (charge state); **f** GCD curves in ZnSO<sub>4</sub> and ZnMg-0.1 electrolyte at 0.5–5.0 A g<sup>-1</sup>; **g** longevity performance in ZnSO<sub>4</sub> and ZnMg-0.1 electrolyte at 5.0 A g<sup>-1</sup>. Reproduced with permission from [86], Copyright 2021, Wiley–VCH

the electrochemical capacitance of ZIHCs. The ZIHC composed of ZnSO<sub>4</sub>, ZnCl<sub>2</sub>, and ZnAc<sub>2</sub> as the electrolyte, TiN as cathode, and metallic Zn as anodes was constructed [45] to investigate the consequence of the electrochemical performance of anion carrier. The TiN-SO<sub>4</sub> has the smoothest adsorption process, and the lowest adsorption energy is possessed by SO<sub>4</sub><sup>2-</sup>, which was proven by discrete Fourier transform (DFT) calculation of the adsorption energies of the TiN cathode for the three anions. Meanwhile, the ZIHC with ZnSO<sub>4</sub> electrolyte exhibited the superior electrochemical performance of ultra-high capacitance of 314.5 F g<sup>-1</sup> at 0.2 A g<sup>-1</sup> after 10,000 cycles and high capacity retention over 83.92% after resting for 500 h; outstanding stability of the TiN-SO<sub>4</sub>

structure improved the self-discharge resistance of the capacitor, which illustrated that capacitance and self-discharge resistance of ZIHCs are significantly affected by different anion types. Currently, electrolyte additives have been effectively applied in improving the electrochemical performance of ZIHCs. Table 2 summarizes the electrochemical properties of electrolyte control in ZIHCs, showing the high efficiency of electrolyte additives in inhibiting side reactions and hindering the formation and growth of zinc dendrites. The unique design of the electrode structure, as well as the modification of the electrolyte, can significantly improve its electrochemical performance. Meanwhile, the choice of suitable electrolytes still leaves room for further exploration.

**Table 2** Summary of electrolyte-controlled electrochemical properties in ZIHCs

Materials	Electrolyte	Voltage range (V)	Capacity	Current density (A g <sup>-1</sup> )	Electrochemical performance	Energy density (W h kg <sup>-1</sup> )	Power density (kW kg <sup>-1</sup> )	Ref.
FL-P	0.2 M ZnCl <sub>2</sub> in Et <sub>4</sub> NBF <sub>4</sub> /PC electrolyte	0–2.5	363.9 F g <sup>-1</sup>	0.2	/	315.6	23.6	[48]
FCNSs	0.2 M Zn(CF <sub>3</sub> SO <sub>3</sub> ) <sub>2</sub> in EMIMCF <sub>3</sub> SO <sub>3</sub>	0.1–2.4	300 F g <sup>-1</sup>	0.1	82% after 35,000 cycles	217	13	[88]
AC	SA-Zn double network hydrogel electrolyte	0–2.4	260.5 mA h g <sup>-1</sup>	0.2	95.4% after 10,000 cycles	286.6	/	[89]
AC	Redox SA-Zn-Br double network hydrogel	0–2.6	654.8 mA h g <sup>-1</sup>	2	87.7% after 5000 cycles	605	/	[90]

## 5 Summary and perspective

In recent years, ZIHCs have been regarded as emerging electronic energy storage devices with good potential and rapid development momentum, combining the powerful cycling stability of traditional supercapacitors while inheriting the superiority of zinc-ion batteries, including abundant resources, environmental protection, high theoretical capacity, and cost-effectiveness. In this work, we report the recent regulated preparation and modification of carbon cathodes for ZIHC (e.g., AC, BC, PC, and HDC); property improvement measures, such as coating, electrolyte ion regulation, electrode structure design to inhibit the formation and growth of zinc dendrites and possible side reactions, have been carried out to improve ZIHCs electrochemical performance.

Although significant breakthroughs have been made in exploring ZIHCs with carbon-based electrodes, the instability of the electrochemical performance and side reactions in the electrolyte system hinder the concrete application of ZIHCs as excellent performance energy storage devices. Therefore, rational structural control and morphology control of carbon-based materials are crucial for high-performance ZIHCs. In addition, the investigation of electrolytes for ZIHCs is now at the very beginning stage; the development of high-performance ZIHCs is inseparable from an electrolyte system with high voltage and excellent stability. As a result, it is worthwhile to strengthen the research on the mechanism of the electrolyte and build a stable electrolyte to reduce the effect of the side reaction of zinc anode.

The future exploration of ZIHCs carbon-based electrodes can be deepened from the following directions. The electrochemical performance of ZIHCs is closely related to the porosity of carbon-based materials. Building a porous structure can enhance the ion adsorption–desorption capacity of electrolytes, which plays an important role in enhancing capacitance and facilitating ion transport. Besides, heteroatom doping is believed to effectively tune the electrochemical

structure and surface features of carbon; thus, the electrolyte ions have better migration ability on the electrode surface. Familiarity with the effects and working mechanisms of different dopants and the adoption of accurate and repeatable doping strategies are beneficial for obtaining cathode material with excellent performance. Furthermore, carbon-based composites prepared by compounding carbon with various pseudocapacitive materials are a promising new direction for ZIHCs, which have bigger capacitance and larger operating voltage windows than pure carbon alone, but the problems of low rate and low cycle performance cannot be ignored. Therefore, improving the electrochemical stability of carbon-based pseudocapacitive composites and finding ways to suppress side reactions are still challenges.

**Author contribution** As per the journal requirement of more than ten contributors, the required contribution can be briefly stated as follows. Yongpeng Ma: conceptualization, methodology, validation, formal analysis, writing – original draft; Chuanxin Hou: conceptualization, writing – original draft, preparation, methodology, writing – review and editing; Hideo Kimura: conceptualization, resources, and writing – review and editing; Xiubo Xie, Huiyu Jiang, Yuping Zhang, and Xueqin Sun: writing – review and editing; Xiaoyang Yang: methodology, validation; Wei Du: supervision, project administration, writing – review and editing.

**Funding** This work was supported by the National Natural Science Foundation of China (52207249), the Natural Science Foundation of Shandong Province (ZR2022ME089), and the Yantai Basic Research Project (2022JCYJ04).

## Declarations

**Conflict of interest** The authors declare no competing interests.

## References

- Du W, Wang XN, Zhan J, Sun XQ, Kang LT, Jiang FY, Zhang XY, Shao Q, Dong MY, Liu H, Murugadoss V, Guo ZH (2019) Biological cell template synthesis of nitrogen-doped porous hollow

- carbon spheres/MnO<sub>2</sub> composites for high-performance asymmetric supercapacitors. *Electrochim Acta* 296:907–915
2. Dang CC, Mu Q, Xie XB, Sun XQ, Yang XY, Zhang YP, Maganti S, Huang M, Jiang QL, Seok I, Du W, Hou CX (2022) Recent progress in cathode catalyst for nonaqueous lithium oxygen batteries: a review. *Adv Compos Hybrid Mater* 5(2):606–626
  3. Yang WY, Peng DN, Kimura H, Zhang XY, Sun XQ, Pashameah RA, Alzahrani E, Wang B, Guo ZH, Du W, Hou CX (2022) Honeycomb-like nitrogen-doped porous carbon decorated with Co<sub>3</sub>O<sub>4</sub> nanoparticles for superior electrochemical performance pseudo-capacitive lithium storage and supercapacitors. *Adv Compos Hybrid Mater* 5:3146–3157
  4. Hou CX, Tai ZX, Zhao LL, Zhai YJ, Hou Y, Fan YQ, Dang F, Wang J, Liu HK (2018) High performance MnO@C microcages with a hierarchical structure and tunable carbon shell for efficient and durable lithium storage. *J Mater Chem A* 6:9723–9736
  5. Hou CX, Hou Y, Fan YQ, Zhai YJ, Wang Y, Sun ZY, Fan RH, Dang F, Wang J (2018) Oxygen vacancy derived local build-in electric field in mesoporous hollow Co<sub>3</sub>O<sub>4</sub> microspheres promotes high-performance Li-ion batteries. *J Mater Chem A* 6:6967–6976
  6. Hou CX, Wang J, Du W, Wang J, Du Y, Liu C, Zhang J, Hou H, Dang F, Zhao L, Guo Z (2019) One-pot synthesized molybdenum dioxide-molybdenum carbide heterostructures coupled with 3D holey carbon nanosheets for highly efficient and ultrastable cycling lithium-ion storage. *J Mater Chem A* 7:13460–13472
  7. Hou CX, Yang W, Kimur H, Xie X, Zhang X, Sun X, Yu Z, Yang X, Zhang Y, Wang B, Xu B, Sridhar D, Algadi H, Guo Z, Du W (2023) Boosted lithium storage performance by local build-in electric field derived by oxygen vacancies in 3D holey N-doped carbon structure decorated with molybdenum dioxide. *J Mater Sci Technol* 142:185–195
  8. Ma YP, Xie XB, Yang WY, Yu ZP, Sun XQ, Zhang YP, Yang XY, Kimura H, Hou CX, Guo ZH, Du W (2021) Recent advances in transition metal oxides with different dimensions as electrodes for high-performance supercapacitors. *Adv Compos Hybrid Mater* 4(4):906–924
  9. Hou C, Yang W, Xie X, Sun X, Wang J, Naik N, Pan D, Mai X, Guo Z, Dang F, Du W (2021) Agaric-like anodes of porous carbon decorated with MoO<sub>3</sub> nanoparticles for stable ultralong cycling lifespan and high-rate lithium/sodium storage. *J Colloid Interface Sci* 596:396–407
  10. Li B, Guo MH, Chen XQ, Miao YY (2022) Hydrothermally synthesized N and S co-doped mesoporous carbon microspheres from poplar powder for supercapacitors with enhanced performance. *Adv Compos Hybrid Mater* 5:2306–2316
  11. Chen Y, Wu SH, Li XH, Liu MY, Chen Z, Zhang PT, Li SJ (2022) Efficient and stable low-cost perovskite solar cells enabled by using surface passivated carbon as the counter electrode. *J Mater Chem C* 10:1270–1275
  12. Zhang YM, Liu LY, Zhao LL, Hou CX, Huang MN, Algadi H, Li DY, Xia Q, Wang J, Zhou ZR, Han X, Long YX, Li YB, Zhang ZD, Liu Y (2022) Sandwich-like CoMoP<sub>2</sub>/MoP heterostructures coupling N, P co-doped carbon nanosheets as advanced anodes for high-performance lithium-ion batteries. *Adv Compos Hybrid Mater* 5:2601–2610
  13. Wang R, Meng ZH, Yan XM, Tian T, Lei M, Pashameah RA, Abo-Dieff HM, Algadi H, Huang NN, Guo ZH, Tang HL (2023) Tellurium intervened Fe-N codoped carbon for improved oxygen reduction reaction and high-performance Zn-air batterie. *J Mater Sci Technol* 137:215–222
  14. Chen AL, Wang CY, A. Abu Ali O, F. Mahmoud S, Shi YT, Ji YX, Algadi H, M. El-Bahy S, Huang MN, Guo ZH, Cui DP, Wei HG (2022) MXene@nitrogen-doped carbon films for supercapacitor and piezoresistive sensing applications. *Compos A* 163:107174
  15. Wang X, Wei H, Liu X, Du W, Zhao X, Wang X (2019) Novel three-dimensional polyaniline nanothorns vertically grown on buckypaper as high-performance supercapacitor electrode. *Nanotechnology* 30(32)
  16. Ahmed FBM, Khalafallah D, Zhi MJ, Hong ZL (2022) Porous nanoframes of sulfurized NiAl layered double hydroxides and ternary bismuth cerium sulfide for supercapacitor electrodes. *Adv Compos Hybrid Mater* 5:2500–2514
  17. Zhao YL, Liu F, Zhu KJ, Maganti S, Zhao ZY, Bai PK (2022) Three-dimensional printing of the copper sulfate hybrid composites for supercapacitor electrodes with ultra-high areal and volumetric capacitances. *Adv Compos Hybrid Mater* 5:1537–1547
  18. Pathak M, Rout CS (2022) Hierarchical NiCo<sub>2</sub>S<sub>4</sub> nanostructures anchored on nanocarbons and Ti<sub>3</sub>C<sub>2</sub>T<sub>x</sub> MXene for high-performance flexible solid-state asymmetric supercapacitors. *Adv Compos Hybrid Mater* 5:1404–1422
  19. Pu L, Zhang J, Jiresse NKL, Gao YF, Zhou HJ, Naik N, Gao P, Guo ZH (2022) N-doped MXene derived from chitosan for the highly effective electrochemical properties as supercapacitor. *Adv Compos Hybrid Mater* 5:356–369
  20. Li F, Li Q, Kimura H, Xie X, Zhang X, Wu N, Sun X, Xu B, Algadi H, Pashameah R, Alanazi AK, Alzahrani E, Du W, Guo Z, Hou CX (2023) Morphology controllable urchin-shaped bimetallic nickel-cobalt oxide/carbon composites with enhanced electromagnetic wave absorption performance. *J Mater Sci Technol*. <https://doi.org/10.1016/j.jmst.2022.12.003>
  21. Sun Z, Qu KQ, Li JH, Yang S, Yuan BN, Huang ZH, Guo ZH (2021) Self-template biomass-derived nitrogen and oxygen co-doped porous carbon for symmetrical supercapacitor and dye adsorption. *Adv Compos Hybrid Mater* 4:1413–1424
  22. Du W, Wang XN, Ju XY, Xu K, Gao MJ, Zhang XT (2017) Carbonized enteromorpha prolifera with porous architecture and its polyaniline composites as high-performance electrode materials for supercapacitors. *J Electroanal Chem* 802:15–21
  23. Wu D, Xie XB, Zhang JJ, Ma YP, Hou CX, Sun XQ, Yang XY, Zhang YP, Kimura H, Du W (2022) Embedding NiS nanoflakes in electrospun carbon fibers containing NiS nanoparticles for hybrid supercapacitors. *Chem Eng J* 446
  24. Wu D, Xie XB, Ma YP, Zhang JJ, Hou CX, Sun XQ, Yang XY, Zhang YP, Kimura H, Du W (2022) Morphology controlled hierarchical NiS/carbon hexahedrons derived from nitrilotriacetic acid-assembly strategy for high-performance hybrid supercapacitors. *Chem Eng J* 433
  25. Li C, Wu W, Wang P, Zhou W, Wang J, Chen Y, Fu L, Zhu Y, Wu Y, Huang W (2019) Fabricating an aqueous symmetric supercapacitor with a stable high working voltage of 2 V by using an alkaline-acidic electrolyte. *Adv Sci* 6(1):1801665
  26. Dong LB, Ma XP, Li Y, Zhao L, Liu WB, Cheng JY, Xu CJ, Li BH, Yang QH, Kang FY (2018) Extremely safe, high-rate and ultralong-life zinc-ion hybrid supercapacitors. *Eng Storage Mater* 13:96–102
  27. Zhang D, Li L, Gao YH, Wu YC, Deng JP (2021) Carbon-based materials for a new type of zinc-ion capacitor. *ChemElectroChem* 8(9):1541–1557
  28. Hui J, Yan CP, Shi Y, Ma QC, Yang Z (2022) A biomass cathode derived from hyacinth bean for aqueous zinc-ion capacitors. *Ionics* 28(3):1495–1499
  29. Kundu DP, Adams BD, Duffort V, Vajargah SH, Nazar LF (2016) A high-capacity and long-life aqueous rechargeable zinc battery using a metal oxide intercalation cathode. *Nat Eng* 1(10). <https://doi.org/10.1038/nenergy.2016.119>
  30. Xia C, Guo J, Li P, Zhang X, Alshareef HN (2018) Highly stable aqueous zinc-ion storage using a layered calcium vanadium oxide bronze cathode. *Angew Chem Int Ed Engl* 57(15):3943–3948
  31. Blanc LE, Kundu D, Nazar LF (2020) Nazar, scientific challenges for the implementation of Zn-ion batteries. *Joule* 4(4):771–799
  32. Tian YH, Amal R, Wang DW (2016) An aqueous metal-ion capacitor with oxidized carbonnanotubes and metallic zinc electrodes. *Front Energy Res* 4. <https://doi.org/10.3389/fenrg.2016.00034>

33. Xu ZX, Ma RJ, Wang XL (2022) Ultrafast, long-life, high-loading, and wide-temperature zinc ion supercapacitors. *Eng Storage Mater* 46:233–242
34. Zhang YP, Ding P, Wu WB, Kimura H, Shen YH, Wu D, Xie XB, Hou CX, Sun XQ, Yang YX, Du W (2023) Facile synthesis of reduced graphene oxide@Co<sub>3</sub>O<sub>4</sub> composites derived from assisted liquid-phase plasma electrolysis for high-performance hybrid supercapacitors. *Appl Sur Sci* 609
35. Gou Q, Zhao S, Wang J, Li M, Xue J (2020) Recent advances on boosting the cell voltage of aqueous supercapacitors. *Nanomicro Lett* 12(1):98
36. Mohd Abdah MAA, Azman NHN, Kulandaivalu S, Sulaiman Y (2020) Review of the use of transition-metal-oxide and conducting polymer-based fibres for high-performance supercapacitors. *Mater Des* 186
37. Wan F, Zhang LL, Wang XY, Bi SS, Niu ZQ, Chen J (2018) An aqueous rechargeable zinc-organic battery with hybrid mechanism. *Adv Funct Mater* 28(45):1804975
38. Chao D, Ye C, Xie F, Zhou W, Zhang Q, Gu Q, Davey K, Gu L, Qiao SZ (2020) Atomic engineering catalyzed MnO<sub>2</sub> electrolysis kinetics for a hybrid aqueous battery with high power and energy density. *Adv Mater* 32(25):2001894
39. Yin J, Zhang WL, Alhebshi NA, Salah N, Alshareef HN (2021) Electrochemical zinc ion capacitors: fundamentals, materials, and systems. *Adv Eng Mater* 11(21):2100201
40. Lu YY, Li ZW, Bai ZY, Mi HY, Ji CC, Pang H, Yu C, Qiu JS (2019) High energy-power Zn-ion hybrid supercapacitors enabled by layered B/N co-doped carbon cathode. *Nano Energy* 66
41. Sun QK, Zhou LJ, Lu LJ, Zhou GQ, Chen JP (2018) ReconFigurable high-resolution microwave photonic filter based on dual-ring-assisted MZIs on the Si<sub>3</sub>N<sub>4</sub> platform. *IEEE Photo J* 10(6):1–12
42. Zhang Y, Liu Y, Wu M, Wang H, Wu L, Xu B, Zhou W, Fan X, Shao J, Yang T (2020) MicroRNA-664a-5p promotes osteogenic differentiation of human bone marrow-derived mesenchymal stem cells by directly downregulating HMGA<sub>2</sub>. *Biochem Biophys Res Commun* 521(1):9–14
43. Zheng YW, Zhao W, Jia DD, Liu Y, Cui L, Wei D, Zheng RK, Liu JQ (2020) Porous carbon prepared via combustion and acid treatment as flexible zinc-ion capacitor electrode material. *Chem Eng J* 387
44. Li ZW, Chen DH, An YF, Chen CL, Wu LY, Chen ZJ, Sun Y, Zhang XG (2020) Flexible and anti-freezing quasi-solid-state zinc ion hybrid supercapacitors based on pencil shavings derived porous carbon. *Eng Storage Mater* 28:307–314
45. Huang Z, Wang T, Song H, Li X, Liang G, Wang D, Yang Q, Chen Z, Ma L, Liu Z, Gao B, Fan J, Zhi C (2021) Effects of anion carriers on capacitance and self-discharge behaviors of zinc-ion capacitors. *Angew Chem Int Ed Engl* 60(2):1011–1021
46. Gong XF, Chen JW, Lee PS (2021) Zinc-ion hybrid supercapacitors: progress and future perspective. *Batteries Supercaps* 4(10):1529–1546
47. Wu SL, Chen YT, Jiao TP, Zhou J, Cheng JY, Liu B, Yang SR, Zhang KL, Zhang WJ (2019) An aqueous Zn-ion hybrid supercapacitor with high energy density and ultrastability up to 80 000 Cycles. *Adv Eng Mater* 9(47):1902915
48. Huang ZD, Chen A, Mo FN, Liang GJ, Li XL, Yang Q, Guo Y, Chen Z, Li Q, Dong BB, Zhi CY (2020) Phosphorene as cathode material for high-voltage, anti-self-discharge zinc ion hybrid capacitors. *Adv Eng Mater* 10(24):2001024
49. Wang JC, Kaskel S (2012) KOH activation of carbon-based materials for energy storage. *J Mater Chem* 22(45):23710
50. Xie XB, Wang YK, Sun XQ, Yu RH, Du W (2023) Optimizing impedance matching by a dual-carbon Co-regulation strategy of Co<sub>3</sub>O<sub>4</sub>@rGO/celery stalks derived carbon composites for excellent microwave absorption. *J Mater Sci Technol* 133:1–11
51. Gao S, Zhao X, Fu Q, Zhang T, Zhu J, Hou F, Ni J, Zhu C, Li T, Wang Y, Murugadoss V (2022) Highly transmitted silver nanowires-SWCNTs conductive flexible film by nested density structure and aluminum-doped zinc oxide capping layer for flexible amorphous silicon solar cell. *J Mater Sci Technol* 126:152–160. <https://doi.org/10.1016/j.jmst.2022.03.012>
52. Xie XB, Qin YT, Wang YK, Wang YX, Feng XY, Chen MN, Ban QF, Hideo K, Du W (2022) Wide microwave absorption bandwidth of the puffed-rice-based carbon obtained at 950 °C. *J Mater Sci Mater Electron* 33(17):14134–14143
53. Wang H, Wang M, Tang YB (2018) A novel zinc-ion hybrid supercapacitor for long-life and low-cost energy storage applications. *Eng Storage Mater* 13:1–7
54. Zhang P, Li Y, Wang G, Wang F, Yang S, Zhu F, Zhuang X, Schmidt OG, Feng X (2019) Zn-ion hybrid micro-supercapacitors with ultrahigh areal energy density and long-term durability. *Adv Mater* 31(3):1806005
55. An GH (2020) Ultrafast long-life zinc-ion hybrid supercapacitors constructed from mesoporous structured activated carbon. *Appl Surf Sci* 530
56. Yu PF, Zeng Y, Zeng YX, Dong HW, Hu H, Liu YL, Zheng MT, Xiao Y, Lu XH, Liang YR (2019) Achieving high-energy-density and ultra-stable zinc-ion hybrid supercapacitors by engineering hierarchical porous carbon architecture. *Electrochim Acta* 327
57. Wang DW, Pan ZM, Lu ZM (2020) From starch to porous carbon nanosheets: promising cathodes for high-performance aqueous Zn-ion hybrid supercapacitors. *Microporous Mesoporous Mater* 306
58. Pan ZM, Lu ZM, Xu L, Wang DW (2020) A robust 2D porous carbon nanoflake cathode for high energy-power density Zn-ion hybrid supercapacitor applications. *Appl Surf Sci* 510
59. Jiang CH, Zou ZM (2020) Waste polyurethane foam filler-derived mesoporous carbons as superior electrode materials for EDLCs and Zn-ion capacitors. *Diamond Relat Mater* 101
60. Chen SM, Ma LT, Zhang K, Kamruzzaman M, Zhi CY, Zapien JA (2019) A flexible solid-state zinc ion hybrid supercapacitor based on co-polymer derived hollow carbon spheres. *J Mater Chem A* 7(13):7784–7790
61. Lee YG, An GH (2020) Synergistic effects of phosphorus and boron co-incorporated activated carbon for ultrafast zinc-ion hybrid supercapacitors. *ACS Appl Mater Inter* 12(37):41342–41349
62. Liu PG, Gao Y, Tan YY, Liu WF, Huang YP, Yan J, Liu KY (2019) Rational design of nitrogen doped hierarchical porous carbon for optimized zinc-ion hybrid supercapacitors. *Nano Res* 12(11):2835–2841
63. Jian Z, Yang NJ, Vogel M, Leith S, Schönherr H, Jiao TP, Zhang WJ, Müller J, Butz B, Jiang X (2020) Flexible diamond fibers for high-energy-density zinc-ion supercapacitors. *Adv Eng Mater* 10(44):2002202
64. Li Y, Lu PF, Shang P, Wu LS, Wang X, Dong YF, He RH, Wu ZS (2021) Pyridinic nitrogen enriched porous carbon derived from bimetal organic frameworks for high capacity zinc ion hybrid capacitors with remarkable rate capability. *J Eng Chem* 56:404–411
65. Wang G, Wang H, Lu X, Ling Y, Yu M, Zhai T, Tong Y, Li Y (2014) Solid-state supercapacitor based on activated carbon cloths exhibits excellent rate capability. *Adv Mater* 26(17): 2676–82, 2615
66. Zhao P, Yang BJ, Chen JT, Lang JW, Zhang TY, Yan XB (2020) A safe, high-performance, and long-cycle life zinc-ion hybrid capacitor based on three-dimensional porous activated carbon. *Acta Phys Chim Sin* 36(2):1904050
67. Tang H, Yao JJ, Zhu YR (2021) Recent developments and future prospects for zinc-ion hybrid capacitors: a review. *Adv Eng Mater* 11(14):2003994
68. He L, Liu Y, Li CY, Yang DZ, Wang WG, Yan WQ, Zhou WB, Wu ZX, Wang LL, Huang QH, Zhu YS, Chen YH, Fu LJ, Hou XH, Wu YP (2019) A low-cost Zn-based aqueous supercapacitor with high energy density. *ACS Appl Eng Mater* 2(8):5835–5842
69. Zou ZM, Luo XL, Wang L, Zhang Y, Xu ZJ, Jiang CH (2021) Highly mesoporous carbons derived from corn silks as high



- performance electrode materials of supercapacitors and zinc ion capacitors. *J Eng Storage* 44
70. Liu H, Liu XX, Li W, Guo X, Wang Y, Wang GX, Zhao DY (2017) Porous carbon composites for next generation rechargeable lithium batteries. *Adv Eng Mater* 7(24):1700283
  71. Kumar R, Sahoo S, Joanni E, Singh RK, Maegawa K, Tan WK, Kawamura G, Kar KK, Matsuda A (2020) Heteroatom doped graphene engineering for energy storage and conversion. *Mater Today* 39:47–65
  72. Zhang H, Liu Q, Fang Y, Teng C, Liu X, Fang P, Tong Y, Lu X (2019) Boosting Zn-ion energy storage capability of hierarchically porous carbon by promoting chemical adsorption. *Adv Mater* 31(44):1904948
  73. Deng XY, Li JJ, Shan Z, Sha JW, Ma LY (2020) A N, O co-doped hierarchical carbon cathode for high-performance Zn-ion hybrid supercapacitors with enhanced pseudocapacitance. *J Mater Chem A* 8(23):11617–11625
  74. Agnoli S, Favaro M (2016) Doping graphene with boron: a review of synthesis methods, physicochemical characterization, and emerging applications. *J Mater Chem A* 4(14):5002–5025
  75. Siahrostami S, Tripkovic V, Lundgaard KT, Jensen KE, Hansen HA, Hummelshoj JS, Myrdal JS, Vegge T, Norskov JK, Rossmeisl J (2013) First principles investigation of zinc-anode dissolution in zinc-air batteries. *Phys Chem Chem Phys* 15(17):6416–6421
  76. Liu M, Pu X, Cong Z, Liu Z, Liu T, Chen Y, Fu J, Hu W, Wang ZL (2019) Resist-dyed textile alkaline Zn microbatteries with significantly suppressed Zn dendrite growth. *ACS Appl Mater Inter* 11(5):5095–5106
  77. Yang Q, Liang G, Guo Y, Liu Z, Yan B, Wang D, Huang Z, Li X, Fan J, Zhi C (2019) Do zinc dendrites exist in neutral zinc batteries: a developed electrohealing strategy to in situ rescue in-service batteries. *Adv Mater* 31(43):1903778
  78. Zeng Y, Zhang X, Qin R, Liu X, Fang P, Zheng D, Tong Y, Lu X (2019) Dendrite-free zinc deposition induced by multifunctional CNT frameworks for stable flexible Zn-ion batteries. *Adv Mater* 31(36):1903675
  79. Zhang J, Han X, Wu XW, Liu Y, Cui Y (2019) Chiral DHIP- and pyrrolidine-based covalent organic frameworks for asymmetric catalysis. *ACS Sustainable Chem Eng* 7(5):5065–5071
  80. Guo J, Ming J, Lei YJ, Zhang WL, Xia C, Cui Y, Alshareef HN (2019) Artificial solid electrolyte interphase for suppressing surface reactions and cathode dissolution in aqueous zinc ion batteries. *ACS Energy Lett* 4(12):2776–2781
  81. Zhu QS, Zhao Y, Miao BJ, M. Abo-Dief H, Qu MC, Pashameah RA, Xu BB, Huang MA, Algadi H, Liu XH, Guo ZH, (2022) Hydrothermally synthesized ZnO-RGO-PPy for water-borne epoxy nanocomposite coating with anticorrosive reinforcement. *Prog Org Coat* 172
  82. Lee BS, Cui S, Xing X, Liu H, Yue X, Petrova V, Lim HD, Chen R, Liu P (2018) Dendrite suppression membranes for rechargeable zinc batteries. *ACS Appl Mater Interfaces* 10(45):38928–38935
  83. Dong LB, Yang W, Yang W, Tian H, Huang YF, Wang XL, Xu CJ, Wang CY, Kang FY, Wang GX (2020) Flexible and conductive scaffold-stabilized zinc metal anodes for ultralong-life zinc-ion batteries and zinc-ion hybrid capacitors. *Chem Eng J* 384
  84. Liu K, Pei A, Lee HR, Kong B, Liu N, Lin D, Liu Y, Liu C, Hsu PC, Bao Z, Cui Y (2017) Lithium metal anodes with an adaptive “solid-liquid” interfacial protective layer. *J Am Chem Soc* 139(13):4815–4820
  85. Zhao ZM, Zhao JW, Hu ZL, Li JD, Li JJ, Zhang YJ, Wang C, Cui GL (2019) Long-life and deeply rechargeable aqueous Zn anodes enabled by a multifunctional brightener-inspired interphase. *Energy Environ Sci* 12(6):1938–1949
  86. Wang PJ, Xie XS, Xing ZY, Chen XH, Fang GZ, Lu BG, Zhou J, Liang SQ, Fan HJ (2021) Mechanistic insights of Mg<sup>2+</sup>-electrolyte additive for high-energy and long-life zinc-ion hybrid capacitors. *Adv Eng Mater* 11(30):2101158
  87. Owusu KA, Pan X, Yu R, Qu L, Liu Z, Wang Z, Tahir M, Haider WA, Zhou L, Mai L (2020) Introducing Na<sub>2</sub>SO<sub>4</sub> in aqueous ZnSO<sub>4</sub> electrolyte realizes superior electrochemical performance in zinc-ion hybrid capacitor. *Mater Today Energ* 18:100529
  88. Zhou HT, Liu C, Wu JC, Liu MH, Zhang D, Song HL, Zhang XY, Gao HQ, Yang JH, Chen D (2019) Boosting the electrochemical performance through proton transfer for the Zn-ion hybrid supercapacitor with both ionic liquid and organic electrolytes. *J Mater Chem A* 7(16):9708–9715
  89. Han L, Huang HL, Fu XB, Li JF, Yang ZL, Liu XJ, Pan LK, Xu M (2020) A flexible, high-voltage and safe zwitterionic natural polymer hydrogel electrolyte for high-energy-density zinc-ion hybrid supercapacitor. *Chem Eng J* 392
  90. Han L, Huang HL, Li JF, Zhang XL, Yang ZL, Xu M, Pan LK (2020) A novel redox bromide-ion additive hydrogel electrolyte for flexible Zn-ion hybrid supercapacitors with boosted energy density and controllable zinc deposition. *J Mater Chem A* 8(30):15042–15050

**Publisher's Note** Springer Nature remains neutral with regard to jurisdictional claims in published maps and institutional affiliations.

Springer Nature or its licensor (e.g. a society or other partner) holds exclusive rights to this article under a publishing agreement with the author(s) or other rightsholder(s); author self-archiving of the accepted manuscript version of this article is solely governed by the terms of such publishing agreement and applicable law.